AMERICAN SOCIETY FOR MICROBIOLOGY | Infection and Immunity®

CELLULAR MICROBIOLOGY: PATHOGEN-HOST CELL MOLECULAR INTERACTIONS

Leishmania donovani Metacyclic Promastigotes Impair Phagosome Properties in Inflammatory Monocytes

Christine Matte,[a] Guillermo Arango Duque,[a]* Albert Descoteaux[a]

[a]INRS – Centre Armand-Frappier Santé Biotechnologie, Université du Québec, Laval, Quebec, Canada

ABSTRACT Leishmaniasis, a debilitating disease with clinical manifestations ranging from self-healing ulcers to life-threatening visceral pathologies, is caused by protozoan parasites of the *Leishmania* genus. These professional vacuolar pathogens are transmitted by infected sand flies to mammalian hosts as metacyclic promastigotes and are rapidly internalized by various phagocyte populations. Classical monocytes are among the first myeloid cells to migrate to infection sites. Recent evidence shows that recruitment of these cells contributes to parasite burden and the establishment of chronic disease. However, the nature of *Leishmania*-inflammatory monocyte interactions during the early stages of host infection has not been well investigated. Here, we aimed to assess the impact of *Leishmania donovani* metacyclic promastigotes on antimicrobial responses within these cells. Our data showed that inflammatory monocytes are readily colonized by *L. donovani* metacyclic promastigotes, while infection with *Escherichia coli* is efficiently cleared. Upon internalization, metacyclic promastigotes inhibited superoxide production at the parasitophorous vacuole (PV) through a mechanism involving exclusion of NADPH oxidase subunits gp91^{phox} and p47^{phox} from the PV membrane. Moreover, we observed that unlike phagosomes enclosing zymosan particles, vacuoles containing parasites acidify poorly. Interestingly, whereas the parasite surface coat virulence glycolipid lipophosphoglycan (LPG) was responsible for the inhibition of PV acidification, impairment of the NADPH oxidase assembly was independent of LPG and GP63. Collectively, these observations indicate that permissiveness of inflammatory monocytes to *L. donovani* may thus be related to the ability of this parasite to impair the microbicidal properties of phagosomes.

KEYWORDS *Leishmania*, NADPH oxidase, acidification, inflammatory monocytes, phagosomes, virulence factors

Monocytes are circulating mononuclear phagocytes that are critical orchestrators of the innate immune response to sterile and microbial inflammation (1, 2). They primarily originate from bone marrow myeloid progenitor cells and enter the circulation to infiltrate organs such as the liver and spleen. Monocytes can be classical (Ly6C^{hi}) or nonclassical (Ly6C^{lo}), a dichotomy that allows them to originate distinct macrophage subsets (3, 4). Under physiological conditions, Ly6C^{hi} monocytes monitor extravascular tissues and present antigens to lymphocytes in lymph nodes. Inflammatory signals such as pathogen-derived molecules not only trigger myeloid differentiation into Ly6C^{hi} monocytes but also their CCL2 chemokine-mediated migration to the injury site (5). There, these cells ingest microbes, release inflammatory molecules, and differentiate into macrophages and dendritic cells (1, 6). The importance of Ly6C^{hi} monocytes in antibacterial defense is channeled through their ability to phagocytose and kill pathogens (1, 6–8). At the cellular level, phagosome maturation is driven by sequential soluble *N*-ethylmaleimide-sensitive factor attachment protein receptors (SNARE)-mediated interactions with endosomes and lysosomes (9, 10). This ensues in assembly of the NADPH and NOS2 oxidases on the phagosome membrane,

Citation Matte C, Arango Duque G, Descoteaux A. 2021. *Leishmania donovani* metacyclic promastigotes impair phagosome properties in inflammatory monocytes. Infect Immun 89:e00009-21. https://doi.org/10.1128/IAI.00009-21.

Editor Jeroen P. J. Saeij, UC Davis School of Veterinary Medicine

Address correspondence to Albert Descoteaux, albert.descoteaux@inrs.ca.

* Present address: Guillermo Arango Duque, Université de Montréal, Montréal, Canada.

Received 5 January 2021
Returned for modification 5 March 2021
Accepted 7 April 2021
Accepted manuscript posted online 19 April 2021
Published 16 June 2021

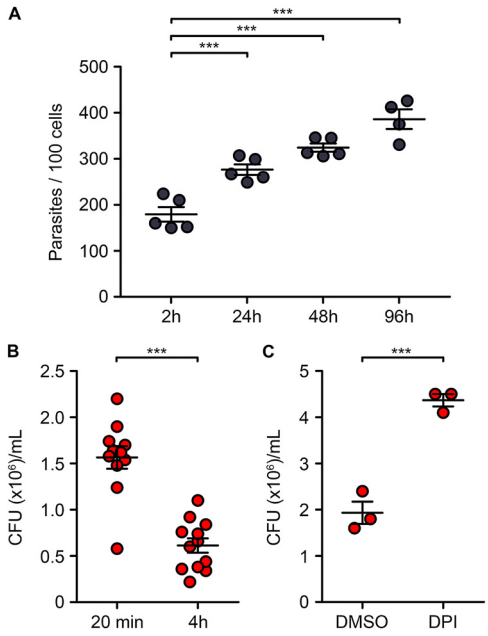

FIG 1 Inflammatory monocytes are permissive to *L. donovani* metacyclic promastigotes replication. Bone marrow cells from C57BL/6 mice were incubated for 3 days in the presence of LCM as a source of CSF-1. Nonadherent cells were seeded in chambers mounted on Permanox slides and stimulated for 3 h with 100 U/ml IFN-γ. Cells were then incubated with serum-opsonized *L. donovani* LV9 metacyclic promastigotes. (A) After 2 h, nonattached/noninternalized parasites were removed by washing, and intracellular parasitemia was assessed at the indicated time points by counting the number of parasites per 100 cells upon staining with the Hema 3 staining kit. (B and C) Inflammatory monocytes were left untreated (B) or treated for 1 h with the NADPH oxidase inhibitor DPI (10 μM) or vehicle drug (DMSO; 0.1%) (C) and then infected with bacteria (*E. coli* DH1; OD_{660}, 0.6; bacteria-to-cell ratio of 20:1) for 20 min. Noninternalized bacteria were removed by washing and via incubation in the presence of 5 μg/ml gentamicin for 20 min (B and C) or 4 h (B), after which the amount of viable intracellular bacteria was assessed through lysis, serial dilutions, and counting of CFU on agar plates. The means $\pm$ SEM of data from two independent experiments representative of a total of four experiments (A), from four independent experiments (B), or from one experiment representative of two experiments (C) are shown. ***, $P < 0.001$ according to a one-way ANOVA with Bonferroni *post hoc* test (A) or a two-tailed, unpaired *t* test (B and C).

which promotes the intraluminal synthesis of the highly microbicidal reactive oxygen (ROS) and nitrogen (RNS) species, respectively (8, 10). Importantly, progressive acidification of the phagosome through the activity of the vacuolar ATPase (v-ATPase) promotes the function of pH-sensitive hydrolytic enzymes (11).

While Ly6C^{hi} monocytes mount a timely and effective response to injury, their persistent accrual may lead to excessive inflammation and organ damage (1). Similarly, Ly6C^{hi} monocytes have been reported to control (12, 13) or exacerbate (14–16) infection by protozoan parasites of the *Leishmania* genus. These parasites cause a group of anthropozoonoses called leishmaniases that are transmitted to mammalian hosts via the inoculation of metacyclic promastigotes by phlebotomine sand flies (17, 18). There, promastigotes are internalized into parasitophorous vacuoles (PV) by host phagocytes and differentiate into amastigotes, which, in turn, propagate infection and disease. Studies in macrophages have revealed that metacyclic promastigotes build their intracellular niche using an armament of abundant glycosylphosphatidylinositol (GPI)-anchored virulence-associated glycoconjugates such as the glycolipid lipophosphoglycan (LPG) and the metalloprotease GP63. These components of the promastigote surface coat were shown to alter phagosome maturation and inhibit acquisition of microbicidal properties, contributing to the colonization of host cells by *Leishmania* promastigotes (19–29).

When *Leishmania major* or *Leishmania amazonensis* are inoculated into the dermis, interferon gamma (IFN-γ)- and CCL2-mediated recruitment of Ly6C^{hi} monocytes creates

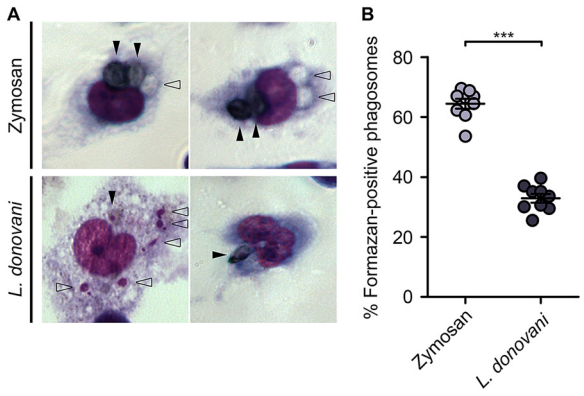

FIG 2 *L. donovani* metacyclic promastigotes downregulate phagosomal ROS production. Inflammatory monocytes were incubated for 15 min with serum-opsonized zymosan particles or *L. donovani* LV9 metacyclic promastigotes, after which nonattached/noninternalized particles were removed by washing. Cells were incubated for 1 h with 1 mg/ml NBT and then stained with the Hema 3 staining kit. Phagosomes positive (full arrowheads) or negative (empty arrowheads) for the presence of formazan deposits were counted. Representative images (A) and the means ± SEM of data from three independent experiments (B) are shown. ***, $P < 0.001$ according to a two-tailed, unpaired *t* test.

a pool of cells that are readily infected by the parasites (15, 16, 30). Similarly, *Leishmania donovani* parasites trigger the expansion of myeloid precursors, which augment the supply of Ly6C^{hi} monocytes to the viscera (14). The early events surrounding the phagocytosis of metacyclic promastigotes by inflammatory monocytes have not been elucidated. In this work, we observed that while inflammatory monocytes are efficient at clearing bacteria, they are highly permissive to *L. donovani* infection. We investigated the impact of *L. donovani* metacyclic promastigotes on inflammatory monocyte antimicrobial effector mechanisms and demonstrated that infection leads to an inhibition of PV oxidative activity and acidification.

RESULTS

***L. donovani* metacyclic promastigotes successfully colonize inflammatory monocytes.** Previous studies have provided evidence that Ly6C-positive inflammatory monocytes serve as permissive host cells for *L. major* during acute primary infection in the skin (30). To investigate how *Leishmania* colonizes these cells, we assessed their permissiveness to *L. donovani* metacyclic promastigotes *in vitro*, as inflammatory monocytes also play a role in promoting parasitemia and susceptibility to visceral leishmaniasis (31, 32). We infected inflammatory monocytes generated from the bone marrow of C57BL/6 mice with serum-opsonized *L. donovani* metacyclic promastigotes, and we assessed parasite burden over a period of 96 h. Consistent with their role as reservoirs that foster parasite burden (31, 32), inflammatory monocytes supported the proliferation of *L. donovani*, which doubled in number within 96 h (Fig. 1A). Classical and intermediate monocytes, compared to their nonclassical counterparts, possess efficient antimicrobial effector mechanisms, including powerful oxidative capacities exerted via NADPH oxidase activity (33–35). In murine infection models, their ability to restrict the growth of pathogens such as *Mycobacterium tuberculosis*, *Salmonella*, or *Listeria* has been well established (8, 35–37). To rule out any potential general defect in the microbicidal response of *in vitro*-generated inflammatory monocytes, we fed them live *Escherichia coli* and assessed bacteria killing over time. In contrast to *L. donovani* metacyclic promastigotes, bacteria were rapidly cleared within 4 h (Fig. 1B). Pretreatment of inflammatory monocyte cultures with the NADPH oxidase inhibitor diphenyleneiodonium (DPI) significantly reduced bactericidal activity compared to vehicle drug alone (dimethyl sulfoxide [DMSO]), confirming the contribution of reactive oxygen species (ROS) in the elimination of internalized microbes by these cells (Fig. 1C).

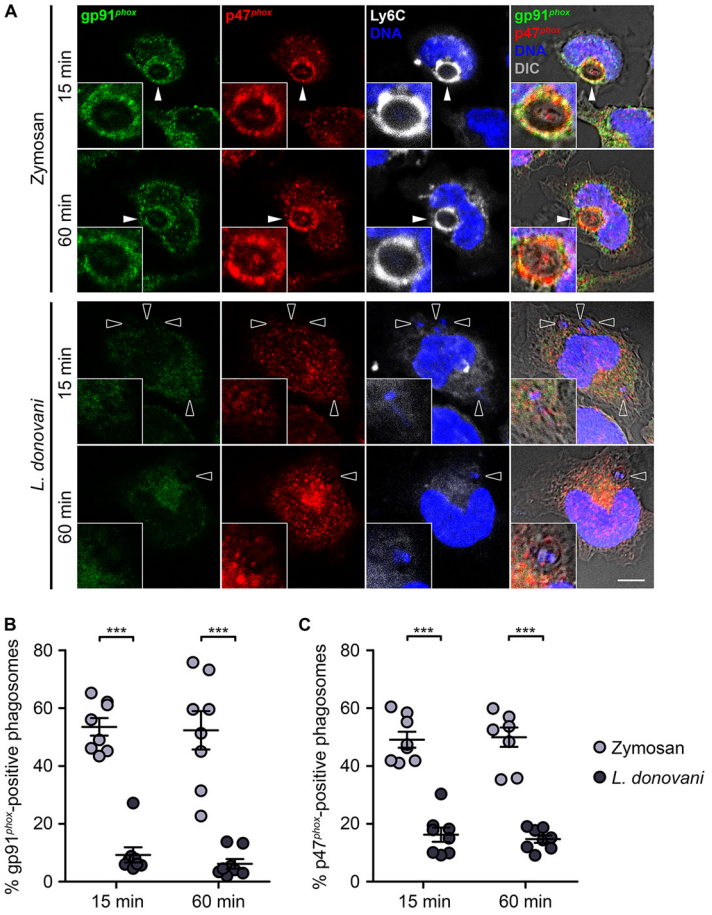

FIG 3 *L. donovani* metacyclic promastigotes impair phagosomal NADPH oxidase assembly. Inflammatory monocytes were incubated for 15 min with serum-opsonized zymosan particles or *L. donovani* WT metacyclic promastigotes, after which nonattached/noninternalized particles were removed by washing. Cells were further incubated for the indicated time points before being fixed, blocked, permeabilized, and stained with DAPI (DNA, blue) and with antibodies against gp91^{phox} (green), p47^{phox} (red), and Ly6C (white). Ly6C-positive monocytes were then visualized by confocal immunofluorescence microscopy to quantify zymosan- and promastigote-containing phagosomes that were positive (full arrowheads) or negative (empty arrowheads) for gp91^{phox} or p47^{phox} recruitment to the membrane. (A to C) Images of representative cells (original magnification) and phagosomes ($\times$2 enlarged insets) are shown (A), along with the means $\pm$ SEM of data from three independent experiments (B and C). Scale bar, 5 μm. DIC, differential interference contrast. ***, $P < 0.001$ according to a one-way ANOVA with Bonferroni *post hoc* test.

***L. donovani* promastigotes prevent assembly of the NADPH oxidase at the PV in inflammatory monocytes.** Given the role of ROS in the antimicrobial activity of inflammatory monocytes, we examined the possibility that *L. donovani* metacyclic promastigotes colonize those cells by interfering with the production of ROS. Inflammatory monocytes were fed opsonized parasites for 15 min and then incubated with nitroblue tetrazolium (NBT), a compound that generates dark formazan deposits upon reduction by superoxide. After 1 h, we detected formazan in 30% of PVs harboring *L. donovani* (Fig. 2). On the other hand, internalization of zymosan led to the generation of formazan in over 65% of phagosomes (Fig. 2). These results indicated that *L. donovani* metacyclic promastigotes impair phagosomal ROS production in inflammatory monocytes. To identify the mechanism underlying the impaired phagosomal ROS production in *L. donovani*-infected inflammatory monocytes, we investigated the assembly of the NADPH oxidase at the PV membrane. The cytosolic component p47^{phox} and the transmembrane subunit gp91^{phox} are integral in mediating NADPH oxidase assembly and function, respectively. While p47^{phox} orchestrates complex formation in

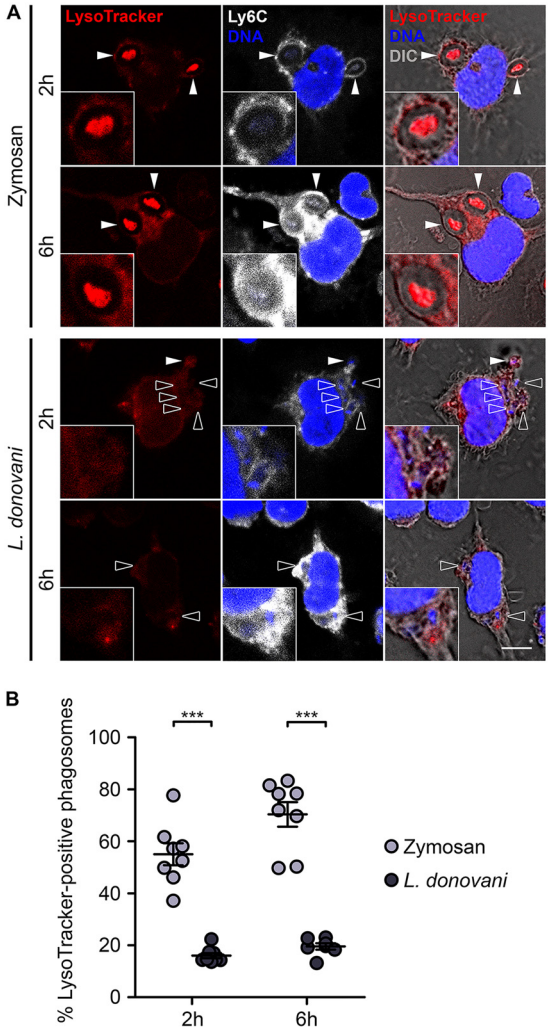

FIG 4 *L. donovani* metacyclic promastigotes prevent phagosomal acidification. Inflammatory monocytes were incubated for 15 min with serum-opsonized zymosan particles or *L. donovani* WT metacyclic promastigotes, after which nonattached/noninternalized particles were removed by washing. Cells were further incubated for up to 6 h with LysoTracker DND-99 (red) added 2 h before the end of each time point. Cells were then fixed, blocked, permeabilized, and stained with DAPI (blue) and for Ly6C (white). Ly6C-positive monocytes were subsequently visualized by confocal immunofluorescence microscopy to quantify the number of phagosomes that were positive (full arrowheads) or negative (empty arrowheads) for LysoTracker fluorescence. (A and B) Images of representative cells (original magnification) and phagosomes (×2 enlarged insets) are shown (A), along with the means ± SEM of data from three independent experiments (B). Scale bar, 5 μm. DIC, differential interference contrast. ***, $P < 0.001$ according to a one-way ANOVA with Bonferroni *post hoc* test.

response to activation by translocating other cytosolic subunits to the membrane, gp91^{phox} catalyzes superoxide production by transferring electrons from NADPH to molecular oxygen (38). Using confocal immunofluorescence microscopy, we monitored the redistribution of each subunit in Ly6C-positive monocytes upon phagocytosis of zymosan versus promastigotes. At 15 and 60 min postinternalization, phagosomes containing zymosan displayed evident recruitment of gp91^{phox} and p47^{phox} (Fig. 3). Interestingly, Ly6C was also detected on the phagosome membrane (Fig. 3A), possibly as a result of plasmalemma internalization during formation and sealing of the phagocytic cup. Conversely, the NADPH oxidase subunits were excluded from the majority of *L. donovani*-harboring PVs (Fig. 3), indicating that metacyclic promastigotes interfere

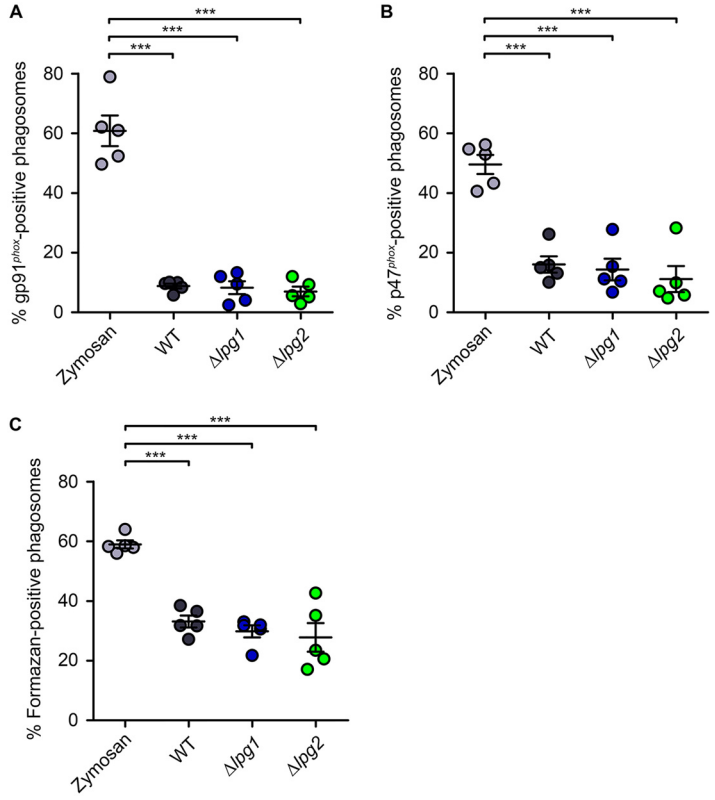

FIG 5 Downregulation of phagosomal ROS production is independent of phosphoglycans. (A to C) Inflammatory monocytes were incubated for 15 min with serum-opsonized zymosan particles or *L. donovani* metacyclic promastigotes (WT, Δ*lpg1*, and Δ*lpg2*), after which nonattached/noninternalized particles were removed by washing. Cells were then further incubated for 1 h before being fixed, blocked, permeabilized, and stained with DAPI (blue) and antibodies against gp91^{phox} (green), p47^{phox} (red), and Ly6C (white). (A and B) Ly6C-positive monocytes were visualized by confocal immunofluorescence microscopy. (C) Alternatively, cells were incubated for 1 h with 1 mg/ml NBT prior to staining with the Hema 3 kit and visualization by light microscopy. Phagosomes were evaluated for gp91^{phox} recruitment (A), p47^{phox} recruitment (B), or the presence of formazan deposits (C). The means ± SEM of data from three (A and B) or two (C) independent experiments are shown. ***, $P < 0.001$ according to a one-way ANOVA with Bonferroni *post hoc* test.

with assembly of the NADPH oxidase to quell ROS production in inflammatory monocytes.

***L. donovani* promastigotes impair PV acidification.** Phagosomal acidification is required for the intracellular elimination of microorganisms by macrophages since lysosomal enzymes are optimally active at acidic pH (39). We previously reported that *L. donovani* and *Leishmania braziliensis* promastigotes inhibit phagosome acidification during the early phases of macrophage infection (40, 41). Hence, we next assessed the potential impact of *L. donovani* on PV acidification in Ly6C-positive inflammatory monocytes using the acidotropic probe LysoTracker DND-99 and confocal microscopy. We used zymosan as a positive control for phagosome acidification. After 2 h, most phagosomes containing zymosan were fluorescent due to protonation of the probe, indicative of an acidic lumen, and the percentage continued to increase over time (Fig. 4). Of note, a general accumulation of acidic vesicles was observed in the cytosol of Ly6C-positive monocytes at 6 h postphagocytosis of zymosan (Fig. 4A). In contrast, *L. donovani* metacyclic promastigotes were enclosed in PVs that were predominantly negative for LysoTracker fluorescence at 2 h and 6 h postinfection (Fig. 4), indicating that these parasites inhibit PV acidification in Ly6C-positive monocytes.

LPG prevents PV acidification but not NADPH oxidase assembly in inflammatory monocytes. We previously reported that LPG and the metalloprotease GP63, two components of the *Leishmania* promastigote surface coat (42, 43), inhibit

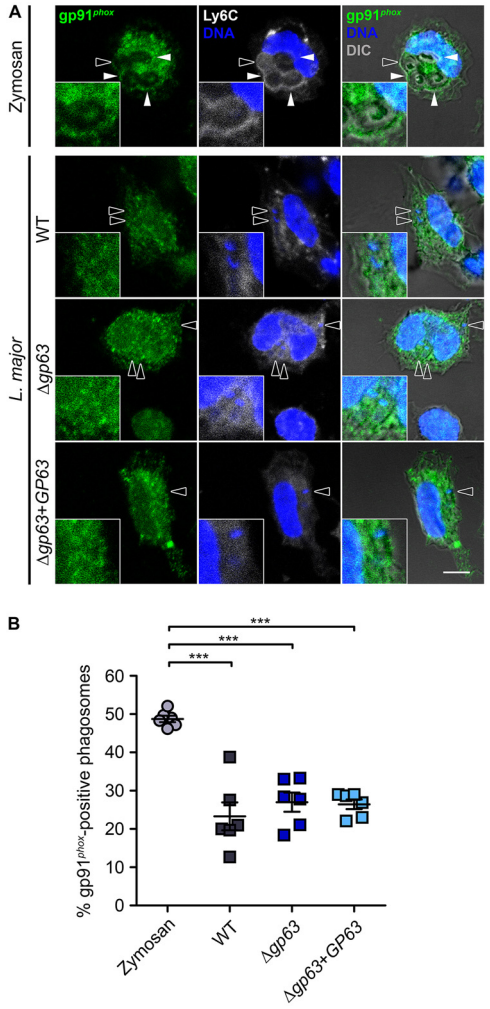

FIG 6 Impairment of the phagosomal recruitment of gp91^{phox} is independent of GP63. Inflammatory monocytes were incubated for 15 min with serum-opsonized zymosan particles or *L. major* NIH S clone A2 metacyclic promastigotes (WT, Δ*gp63*, or Δ*gp63*+*GP63*) at particle-to-cell ratios of 3:1 and 10:1, respectively, after which nonattached/noninternalized particles were removed by washing. Cells were then further incubated for 30 min before being fixed, blocked, permeabilized, and stained with DAPI (DNA, blue) and with antibodies against gp91^{phox} (green) and Ly6C (white). Ly6C-positive monocytes were visualized by confocal immunofluorescence microscopy to quantify zymosan- and promastigote-containing phagosomes that were positive (full arrowheads) or negative (empty arrowheads) for gp91^{phox} recruitment to the membrane. (A and B) Images of representative cells (original magnification) and phagosomes (×2 enlarged insets) are shown (A), along with the means ± SEM of data from three independent experiments (B). Scale bar, 5 μm. DIC, differential interference contrast. ***, $P < 0.001$ according to a one-way ANOVA with Bonferroni *post hoc* test.

phagosomal assembly of the NADPH oxidase in macrophages through distinct mechanisms (23, 26). To determine the potential role of these virulence factors in the inhibition of phagosomal NADPH oxidase assembly in inflammatory monocytes, we first infected these cells with wild type (WT), LPG-deficient Δ*lpg1* mutant, or phosphoglycan [Gal(β1,4)Man(α1)-PO$_4$ repeating unit]-deficient Δ*lpg2* *L. donovani* metacyclic promastigotes (Fig. S1 in the supplemental material). Inflammatory monocytes fed with zymosan were used as positive controls. At 1 h postphagocytosis, we examined the recruitment of gp91^{phox} (Fig. 5A) and p47^{phox} (Fig. 5B) to the PV membrane of Ly6C-positive monocytes. Up to 60% of phagosomes containing zymosan were positive for gp91^{phox} and p47^{phox}. In contrast, only 10% to 15% of phagosomes harboring either WT, Δ*lpg1*, or Δ*lpg2* parasites were positive for gp91^{phox} and p47^{phox}. In agreement with these observations, we found that Δ*lpg1* and Δ*lpg2* *L. donovani* metacyclic promastigotes

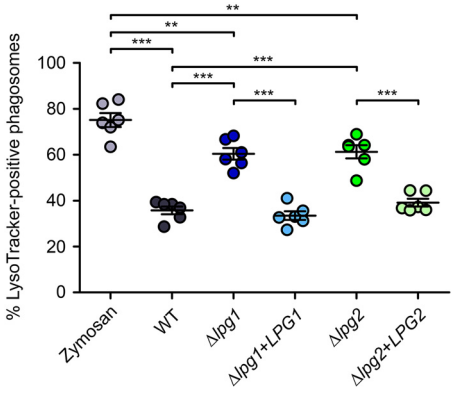

FIG 7 LPG is responsible for the reduction of phagosomal acidification in inflammatory monocytes. Inflammatory monocytes were incubated for 15 min with serum-opsonized zymosan particles or *L. donovani* metacyclic promastigotes (WT, Δ*lpg1*, Δ*lpg2*, Δ*lpg1*+*LPG1*, and Δ*lpg2*+*LPG2*), after which nonattached/noninternalized particles were removed by washing. Cells were then further incubated for 2 h in the presence of LysoTracker DND-99 (red) before being fixed, blocked, permeabilized, and stained with DAPI (blue) and an antibody against Ly6C (white). Ly6C-positive monocytes were finally visualized by confocal immunofluorescence microscopy to assess phagosome acidification. The means ± SEM of data from three independent experiments are shown. ***, $P < 0.001$ according to a one-way ANOVA with Bonferroni *post hoc* test.

dampened the production of superoxide in PVs to the same extent as WT parasites (Fig. 5C). We next assessed the potential role of GP63, given its role in the inhibition of phagosomal NADPH oxidase assembly in *L. major*-infected peritoneal macrophages (29). Since no GP63-deficient parasites are available in *L. donovani*, we used the WT, Δ*gp63*, and Δ*gp63*+*GP63 L. major* lines to infect inflammatory monocytes. Interestingly, in contrast to what is observed in peritoneal macrophages (Fig. S2) (29), absence of GP63 did not abrogate the ability of the metacyclic promastigotes to exclude gp91^{phox} from the PV membrane (Fig. 6). Indeed, only 15% to 20% of inflammatory monocyte phagosomes harboring either of the three *L. major* lines were positive for gp91^{phox} at 30 min postphagocytosis, compared to 50% of phagosomes containing zymosan particles (Fig. 6). Altogether, these results indicate that neither Gal(β1,4)Man(α1)-PO_4-containing glycoconjugates nor GP63 are individually responsible for the inhibition of phagosomal NADPH oxidase assembly in inflammatory monocytes. Of note, the capacity of LPG- and GP63-defective metacyclic promastigotes to prevent phagosomal assembly of the NADPH oxidase is not sufficient to survive in inflammatory monocytes (Fig. S3), consistent with the impact of these two virulence factors on multiple host cell pathways and processes (44, 45).

We previously reported that in macrophages, LPG mediates exclusion of the v-ATPase from *L. donovani*-containing phagosomes (22, 24, 40). Using the Δ*lpg1* and Δ*lpg2* mutants, we verified the role of LPG and other Gal(β1,4)Man(α1)-PO_4-containing parasite glycoconjugates in the inhibition of phagosome acidification in Ly6C-positive monocytes. Inflammatory monocytes fed with zymosan were used as positive controls. As depicted in Fig. 7, in contrast to WT metacyclic promastigotes, the majority of Δ*lpg1* and Δ*lpg2* parasites were present in acidic vacuoles. Finally, complementation of knockout strains (Δ*lpg1*+*LPG1* and Δ*lpg2*+*LPG2*) rescued the capacity of metacyclic promastigotes to prevent PV acidification (Fig. 7). Collectively, these results demonstrate that, akin to what is observed in macrophages (Fig. S4) (40), *L. donovani* metacyclic promastigotes prevent phagosome acidification in inflammatory monocytes in an LPG-dependent manner. The absence of additional PGs in Δ*lpg2* mutants did not affect the frequency of fluorescent PVs, confirming the predominant importance of LPG over other Gal(β1,4)Man(α1)-PO_4-containing glycoconjugates in averting acidification of the newly formed intracellular niche (Fig. 7 and Fig. S4) (40).

DISCUSSION

Leishmania metacyclic promastigotes are deposited by infected sand flies into the dermis of mammals, where they are internalized by various phagocyte populations (30, 46–48). These include inflammatory monocytes, which despite their potent antimicrobial capacities, are highly permissive to *L. major* replication (30). In this study, we aimed to characterize the events that unfold upon phagocytosis of *L. donovani* metacyclic promastigotes by these cells. Our main finding was that *L. donovani* abrogates key antimicrobial processes, namely, phagosomal assembly of the NADPH oxidase and acidification, which may contribute to its capacity to proliferate in inflammatory monocytes. The differential roles of parasite surface glycoconjugates in interfering with these inflammatory monocyte antimicrobial mechanisms are also described.

The outcome of pathogen uptake by phagocytic cells largely depends on the efficiency of microbicidal effector mechanisms within the newly formed phagosome. Generation of ROS at the phagosome represents one of the central host defense mechanisms against infection and depends on the assembly of a functional NADPH oxidase (49, 50). To avoid the harmful consequences of exposure to ROS, pathogens have evolved a panoply of strategies to block assembly and/or resist activity of the NADPH oxidase (49). Hence, *Leishmania* uses diverse mechanisms to reduce exposure to ROS within mammals. One such mechanism is the conversion of toxic ROS through the action of enzymes such as superoxide dismutases (51, 52) and tryparedoxin peroxidase (53, 54). *Leishmania* also interferes with the production of ROS. Induction of higher expression of the macrophage heme oxygenase-1 (55–57) increases heme degradation and was shown to prevent gp91^{phox} maturation (55). Using LPG- and GP63-deficient mutants, we previously reported that in macrophages, disruption of phagosomal membrane lipid microdomains by LPG interferes with the recruitment of cytosolic p47/p67/p40^{phox} heterotrimers (23), whereas recruitment of gp91^{phox} was shown to be inhibited in a GP63-dependent manner (29). Our observation that LPG- and GP63-defective mutants effectively prevented phagosomal assembly of the NADPH oxidase and ROS production to the same extent as WT promastigotes in inflammatory monocytes was thus unexpected and is consistent with the existence of cell type-specific mechanisms for the phagosomal assembly of the NADPH oxidase. Indeed, previous studies revealed the existence of cell type-specific divergence of pathways linking phagocytosis to NADPH oxidase assembly (58). The subcellular distribution of the transmembrane subunit gp91^{phox}, for instance, varies between cell lineages. In resting neutrophils, gp91^{phox} resides in an intracellular pool of granules that are rapidly mobilized to the plasma membrane upon phagocytosis or other stimuli (59, 60). In dendritic cells and macrophages, gp91^{phox} localizes to both the plasma membrane and the endocytic recycling compartment and is replenished through fusion with vesicles of the endocytic compartment via SNAREs such as VAMP8 (26, 60–62). Endothelial cells, on the other hand, maintain a reservoir of gp91^{phox} in the vicinity of the endoplasmic reticulum (63). In inflammatory monocytes, how membrane-bound NADPH oxidase subunits traffic to the phagosome remains to be described. Alternatively, we cannot exclude the possibility that in inflammatory monocytes, absence of LPG in *L. donovani* Δ*lpg1* and Δ*lpg2* mutants was compensated by the action of GP63 on the NADPH oxidase. Conversely, LPG may have endowed *L. major* Δ*gp63* parasites with the capacity to block phagosomal assembly of the NADPH oxidase. Our results also support the concept that vacuolar pathogens such as *Leishmania* have evolved a number of strategies to subvert phagosome oxidative activity based on the biological processes of their various host cells. For instance, it was recently reported that *Leishmania*, which is known to trigger SHP-1 activation (64, 65), inhibits phagosomal activation of NOX2 through the dephosphorylation of p47^{phox} (66). Whether such a mechanism is operational in infected inflammatory monocytes will deserve further investigation.

Phagosomes in classical monocytes and M1 macrophages have been reported to maintain an alkaline or near-neutral pH for up to 30 min postphagocytosis due to consumption of lumen protons by the highly active NADPH oxidase (33, 58). However, in

both cell types, phagosome maturation eventually involves progressive acidification (10). The insertion of LPG into cell membrane bilayers is known to alter phagosome fusion with compartments of the endocytic pathway, leading to a transient arrest in maturation (19, 22, 67). While *L. donovani* promastigote-induced PVs acquire some characteristics of mature phagolysosomes at approximately 5 h postinfection, such as LAMP1 recruitment (68), the exclusion of the proton pump v-ATPase persists up to 24 h (40). This phenotype is congruent with what we observed here in inflammatory monocytes infected with *L. donovani* metacyclic promastigotes, confirming the premise that LPG-mediated inhibition of PV acidification is part of the colonization process of these cells. The observed impairment of PV acidification during the early stages of phagocyte colonization by *L. donovani* and *L. braziliensis* in both inflammatory monocytes and macrophages (40, 41) raises questions on the current model pertaining to the environmental cues associated with the differentiation of promastigotes into amastigotes. Indeed, it is assumed that transformation of promastigotes into amastigotes within the phagosome is mainly triggered by rapid exposure to an acidic environment and an elevated temperature (69, 70). Our data challenge this model, which has been widely used in *in vitro* studies aimed at elucidating the molecular events associated with the promastigote-to-amastigote differentiation process inside phagocytic cells. Clearly, additional studies will be required to elucidate this crucial aspect of *Leishmania* biology.

Prior to this study, the functional biology of inflammatory monocytes in the context of a primary infection with *L. donovani* metacyclic promastigotes had not been addressed in detail. The data presented here demonstrate that, like macrophages, inflammatory monocytes fail to generate robust ROS production upon internalization of *L. donovani* and display a defect in phagosome acidification. Collectively, these findings provide us with a better insight into how inflammatory monocytes foster parasite proliferation and are consistent with the role of these host cells in the establishment of persistent visceral disease (31).

MATERIALS AND METHODS

Ethics statement. Mice were handled in strict accordance with good animal practice as defined by the Canadian Council on Animal Care. Experimental procedures were approved by the Comité Institutionnel de Protection des Animaux of the Centre National de Biologie Expérimentale (protocol 1706-07).

Monocyte cultures. To obtain bone marrow-derived monocytes, bone marrow was flushed from the femurs and tibias of 6- to 8-week-old C57BL/6 mice, treated with 0.17 M NH_4Cl, pH 7.4, for 7 min to lyse red blood cells, and cultured in tissue culture-treated petri dishes in complete medium (Dulbecco's modified Eagle medium with high glucose and L-glutamine (Life Technologies) containing 10% heat-inactivated fetal bovine serum (FBS) (Sigma-Aldrich), 10 mM HEPES, pH 7.4, and penicillin-streptomycin (Life Technologies) supplemented with 15% (vol/vol) L929 cell-conditioned medium (LCM) as a source of colony-stimulating factor-1 (CSF-1) in a 37°C incubator with 5% CO_2. After 3 days, nonadherent cells were collected, transferred to Nunc Lab-Tek 8-well chambers fixed on Permanox plastic slides (Thermo Scientific) in complete medium without LCM, and stimulated with 100 U/ml IFN-γ for 3 h (32). The resulting inflammatory monocyte populations were verified by confocal immunofluorescence microscopy (see below) for Ly6C positivity and the absence of polymorphonuclear cells (Fig. S5).

Parasites cultures. *L. donovani* LV9 (MHOM/ET/67/HU3) and *L. major* NIH S (MHOM/SN/74/Seidman, clone A2) promastigotes were cultured at 26°C in *Leishmania* medium (M199 medium [Sigma-Aldrich] supplemented with 10% heat-inactivated FBS, 10 mM HEPES, pH 7.4, 100 μM hypoxanthine, 5 μM hemin, 3 μM 6-biopterin, 1 μM biotin, and penicillin-streptomycin). The *L. donovani* LV9 isogenic Δ*lpg1* (LPG-defective) and Δ*lpg2* (PG-defective) mutants, produced via homologous gene replacement using targeting constructions previously described (71, 72), were cultured in the presence of hygromycin B at the respective concentrations of 100 μg/ml and 300 μg/ml. To restore *LPG1* expression, Δ*lpg1* promastigotes were electroporated with pLeishZeo-*LPG1* (73), and complemented parasites (Δ*lpg1*+*LPG1*) were selected with 100 μg/ml zeocin (along with hygromycin B). To restore *LPG2* expression, Δ*lpg2* mutants were electroporated with pLeishNeo-*LPG2* (74), and complemented parasites (Δ*lpg2*+*LPG2*) were selected with 20 μg/ml G418 (in addition to hygromycin B). These parasite lines were regularly verified by agglutination tests and by Western blotting using the phosphoglycan-specific CA7AE antibody (MediMabs) (Fig. S1 in the supplemental material) (73). *L. major* NIH S clone A2 isogenic Δ*gp63* mutants and their complemented counterparts (Δ*gp63*+*GP63*, cultured in the presence of 50 μg/ml G418) have been previously described (75). GP63 expression was routinely assessed by Western blotting using the monoclonal antibody number 235 provided by W. Robert McMaster (data not shown) (76). For

infections, metacyclic promastigotes were enriched from late stationary-phase cultures using Ficoll gradients, as described before (77, 78).

Bacteria-killing assay. Bone marrow-derived monocytes were prepared, adhered, stimulated with IFN-γ, and then infected with bacteria as previously described (79). Briefly, nonopsonized *E. coli* DH1 (optical density at 600 nm [OD_{600}], 0.6) was added to inflammatory monocyte cultures at a ratio of 20:1. Chambers were spun in an Eppendorf 5810 R centrifuge at 1,000$\times$ rpm for 1 min and then transferred to 37°C for 20 min to allow binding and phagocytosis, after which noninternalized bacteria were removed by four washes with phosphate-buffered saline (PBS) containing 5 μg/ml gentamicin (Life Technologies). Cells were further incubated at 37°C for either 20 min or 4 h in complete medium supplemented with 5 μg/ml gentamicin. Upon washing with PBS, bactericidal activity was assessed via lysis with a solution of 1% Triton X-100 (vol/vol, in PBS), serial dilutions (1:2,000 was optimal), plating on agar, incubation for 18 h at 37°C, and counting of CFU per milliliter. Where indicated, inflammatory monocytes were pretreated for 1 h with the NADPH oxidase inhibitor DPI (10 μM) or with vehicle drug (DMSO, 0.1%) before adding bacteria.

Phagocytosis. Bone marrow-derived monocytes were prepared, adhered, and stimulated with IFN-γ as described above. Prior to phagocytosis, zymosan particles and metacyclic promastigotes were washed three times with Hanks' balanced salt solution (HBSS) (Life Technologies), incubated with serum from C5-deficient DBA/2 mice (Charles River Laboratories) for 30 min at 37°C, and washed thrice again. To synchronize phagocytosis, cells were fed opsonized zymosan particles or metacyclic promastigotes in cold complete medium without IFN-γ, spun in a Sorvall RT7 centrifuge for 1 min at 1,000 rpm, and transferred to 37°C to trigger internalization. After 15 min, excess particles or parasites were removed by washing three times with warm medium. Cells were then further incubated in complete medium at 37°C for the indicated times. To monitor phagosome acidification, LysoTracker Red DND-99 reagent (Molecular Probes; diluted 1:2,000) was added to cultures 2 h before the end of the indicated time points.

Light microscopy. To detect superoxide production, inflammatory monocytes fed zymosan particles or infected with metacyclic promastigotes as described above were incubated with 1 mg/ml nitroblue tetrazolium (Molecular Probes) for 1 h at 37°C. For parasite survival and proliferation analyses, cells were infected for 2 h with metacyclic promastigotes, washed to remove noninternalized parasites, and then incubated for the indicated times. Permanox plastic slides were detached from the 8-well chambers, stained with the Hema 3 stat pack (Fisher Scientific), and finally covered with coverslips mounted on Fluoromount-G (SouthernBiotech) prior to sealing with nail polish. A minimum of 100 phagosomes per experimental replicate were examined on a Nikon Eclipse E800 microscope. Images were taken using a Leica DM4000 B microscope equipped with a Leica DFC320 digital camera.

Confocal immunofluorescence microscopy. After phagocytosis and incubation for the indicated times, inflammatory monocytes were washed with PBS, fixed with 2% paraformaldehyde (PFA; Canemco and Mirvac) for 20 min, and then simultaneously blocked and permeabilized in 0.1% Triton X-100, 1% bovine serum albumin, 20% normal goat serum, 6% nonfat dry milk, and 50% FBS for 20 min. For the visualization of NADPH oxidase subunit recruitment, cells were sequentially incubated with a solution containing mouse anti-gp91^{phox} (BD Transduction; clone 53; diluted 1:70) and rabbit anti-p47^{phox} (Upstate; catalog no. 07-500; diluted 1:100) antibodies for 2 h, followed by a combination of Alexa Fluor 488-conjugated goat anti-mouse IgG and Alexa Fluor 568-conjugated goat anti-rabbit IgG (Molecular Probes; diluted 1:500) for 30 min, and finally with a mixture of Alexa Fluor 647-conjugated rat anti-mouse Ly6C antibody (BioLegend; clone HK1.4; diluted 1:500) and 4′,6-diamidino-2-phenylindole (DAPI) (Molecular Probes) for 30 min. For phagosome acidification analyses, after fixation and permeabilization, cells were only labeled with DAPI and Ly6C antibody for 30 min. Cells were washed three times with PBS between each incubation, and all steps were performed at room temperature. After staining, Permanox slides were detached from the 8-well chambers and covered with coverslips mounted on Fluoromount-G prior to sealing with nail polish. Fluorescence analyses were performed with a Plan Apochromat $\times$63 oil immersion differential interference contrast (DIC) 1.4 NA objective on a Zeiss LSM780 confocal microscope (Carl Zeiss Microimaging). Images were acquired in plane scanning mode and were minimally and equally processed using Carl Zeiss ZEN software. For each experimental replicate, 100 to 400 phagosomes in Ly6C-positive cells were examined.

Statistical analysis. Univariate scatterplot graphs, presenting data as means $\pm$ standard error of the mean (SEM), were prepared using the GraphPad Prism software. Statistical significance was assessed using either one-way analysis of variance (ANOVA) followed by Bonferroni *post hoc* tests or using a two-tailed, unpaired *t* test (**, $P < 0.01$; ***, $P < 0.001$).

SUPPLEMENTAL MATERIAL

Supplemental material is available online only.

SUPPLEMENTAL FILE 1, PDF file, 2.8 MB.

ACKNOWLEDGMENTS

This work was supported by Canadian Institutes of Health Research (CIHR) grant MOP-125990 to A.D.

A.D. is the holder of the Tier 1 Canada Research Chair on the Biology of intracellular parasitism.

We are grateful to K. Heinonen for advice on the generation of bone marrow-derived inflammatory monocytes and J. Tremblay for assistance with confocal microscopy experiments.

C.M., G.A.D., and A.D. conceived and designed the experiments. C.M. and G.A.D. performed the experiments. C.M., G.A.D., and A.D. analyzed the data. C.M., G.A.D., and A.D. wrote the paper. All authors discussed the findings and commented on the manuscript.

We declare no competing financial interests.

REFERENCES

1. Kratofil Rachel M, Kubes P, Deniset Justin F. 2017. Monocyte conversion during inflammation and injury. Arterioscler Thromb Vasc Biol 37:35–42. https://doi.org/10.1161/ATVBAHA.116.308198.
2. Webster SJ, Daigneault M, Bewley MA, Preston JA, Marriott HM, Walmsley SR, Read RC, Whyte MKB, Dockrell DH. 2010. Distinct cell death programs in monocytes regulate innate responses following challenge with common causes of invasive bacterial disease. J Immunol 185:2968. https://doi.org/10.4049/jimmunol.1000805.
3. Ginhoux F, Jung S. 2014. Monocytes and macrophages: developmental pathways and tissue homeostasis. Nature Rev Immunology 14:392. https://doi.org/10.1038/nri3671.
4. Yang J, Zhang L, Yu C, Yang X-F, Wang H. 2014. Monocyte and macrophage differentiation: circulation inflammatory monocyte as biomarker for inflammatory diseases. Biomarker Res 2:1. https://doi.org/10.1186/2050-7771-2-1.
5. Tsou C-L, Peters W, Si Y, Slaymaker S, Aslanian AM, Weisberg SP, Mack M, Charo IF. 2007. Critical roles for CCR2 and MCP-3 in monocyte mobilization from bone marrow and recruitment to inflammatory sites. J Clinical Invest 117:902–909. https://doi.org/10.1172/JCI29919.
6. Steigbigel RT, Lambert LH, Jr., Remington JS. 1974. Phagocytic and bactericidal properties of normal human monocytes. J Clinical Invest 53:131–142. https://doi.org/10.1172/JCI107531.
7. Shi C, Hohl TM, Leiner I, Equinda MJ, Fan X, Pamer EG. 2011. Ly6G$^+$ neutrophils are dispensable for defense against systemic *Listeria monocytogenes* infection. J Immunol 187:5293. https://doi.org/10.4049/jimmunol.1101721.
8. Serbina NV, Jia T, Hohl TM, Pamer EG. 2008. Monocyte-mediated defense against microbial pathogens. Annu Rev of Immunology 26:421–452. https://doi.org/10.1146/annurev.immunol.26.021607.090326.
9. Dingjan I, Linders PTA, Verboogen DRJ, Revelo NH, Beest M, Bogaart G. 2018. Endosomal and phagosomal SNAREs. Physiological Rev 98:1465–1492. https://doi.org/10.1152/physrev.00037.2017.
10. Levin R, Grinstein S, Canton J. 2016. The life cycle of phagosomes: formation, maturation, and resolution. Immunological Rev 273:156–179. https://doi.org/10.1111/imr.12439.
11. Kissing S, Saftig P, Haas A. 2018. Vacuolar ATPase in phago(lyso)some biology. Int J Med Microbiol 308:58–67. https://doi.org/10.1016/j.ijmm.2017.08.007.
12. Loría-Cervera EN, Andrade-Narvaez F. 2020. The role of monocytes/macrophages in *Leishmania* infection: a glance at the human response. Acta Tropica 207:105456. https://doi.org/10.1016/j.actatropica.2020.105456.
13. Gonçalves R, Zhang X, Cohen H, Debrabant A, Mosser DM. 2011. Platelet activation attracts a subpopulation of effector monocytes to sites of *Leishmania major* infection. J Exp Med 208:1253–1265. https://doi.org/10.1084/jem.20101751.
14. Abidin BM, Hammami A, Stäger S, Heinonen KM. 2017. Infection-adapted emergency hematopoiesis promotes visceral leishmaniasis. PLoS Pathogens 13:e1006422. https://doi.org/10.1371/journal.ppat.1006422.
15. Carneiro MB, Lopes ME, Hohman LS, Romano A, David BA, Kratofil R, Kubes P, Workentine ML, Campos AC, Vieira LQ, Peters NC. 2020. Th1-Th2 cross-regulation controls early *Leishmania* infection in the skin by modulating the size of the permissive monocytic host cell reservoir. Cell Host Microbe 27:752–768.e7. https://doi.org/10.1016/j.chom.2020.03.011.
16. Heyde S, Philipsen L, Formaglio P, Fu Y, Baars I, Höbbel G, Kleinholz CL, Seiß EA, Stettin J, Gintschel P, Dudeck A, Bousso P, Schraven B, Müller AJ. 2018. CD11c-expressing Ly6C$^+$CCR2$^+$ monocytes constitute a reservoir for efficient *Leishmania* proliferation and cell-to-cell transmission. PLoS Pathogens 14:e1007374. https://doi.org/10.1371/journal.ppat.1007374.
17. Killick-Kendrick R, Molyneux D. 1981. Transmission of leishmaniasis by the bite of phlebotomine sandflies: possible mechanisms. Trans Royal Soc Trop Med Hyg 75:152–154. https://doi.org/10.1016/0035-9203(81)90051-1.
18. Kaye P, Scott P. 2011. Leishmaniasis: complexity at the host-pathogen interface. Nature Rev Microbiology 9:604–615. https://doi.org/10.1038/nrmicro2608.
19. Desjardins M, Descoteaux A. 1997. Inhibition of phagolysosomal biogenesis by the *Leishmania* lipophosphoglycan. J Exp Med 185:2061–2068. https://doi.org/10.1084/jem.185.12.2061.
20. Spath GF, Epstein L, Leader B, Singer SM, Avila HA, Turco SJ, Beverley SM. 2000. Lipophosphoglycan is a virulence factor distinct from related glycoconjugates in the protozoan parasite *Leishmania major*. Proc Natl Acad Sci U S A 97:9258–9263. https://doi.org/10.1073/pnas.160257897.
21. Spath GF, Garraway LA, Turco SJ, Beverley SM. 2003. The role(s) of lipophosphoglycan (LPG) in the establishment of *Leishmania major* infections in mammalian hosts. Proc Natl Acad Sci U S A 100:9536–9541. https://doi.org/10.1073/pnas.1530604100.
22. Dermine JF, Goyette G, Houde M, Turco SJ, Desjardins M. 2005. *Leishmania donovani* lipophosphoglycan disrupts phagosome microdomains in J774 macrophages. Cell Microbiol 7:1263–1270. https://doi.org/10.1111/j.1462-5822.2005.00550.x.
23. Lodge R, Diallo TO, Descoteaux A. 2006. *Leishmania donovani* lipophosphoglycan blocks NADPH oxidase assembly at the phagosome membrane. Cell Microbiol 8:1922–1931. https://doi.org/10.1111/j.1462-5822.2006.00758.x.
24. Winberg ME, Holm A, Särndahl E, Vinet AF, Descoteaux A, Magnusson KE, Rasmusson B, Lerm M. 2009. *Leishmania donovani* lipophosphoglycan inhibits phagosomal maturation via action on membrane rafts. Microbes Infect 11:215–222. https://doi.org/10.1016/j.micinf.2008.11.007.
25. Moradin N, Descoteaux A. 2012. *Leishmania* promastigotes: building a safe niche within macrophages. Front Cell Infect Microbiol 2:121. https://doi.org/10.3389/fcimb.2012.00121.
26. Matheoud D, Moradin N, Bellemare-Pelletier A, Shio MT, Hong WJ, Olivier M, Gagnon E, Desjardins M, Descoteaux A. 2013. *Leishmania* evades host immunity by inhibiting antigen cross-presentation through direct cleavage of the SNARE VAMP8. Cell Host Microbe 14:15–25. https://doi.org/10.1016/j.chom.2013.06.003.
27. Arango Duque G, Descoteaux A. 2015. *Leishmania* survival in the macrophage: where the ends justify the means. Curr Opin Microbiol 26:32–40. https://doi.org/10.1016/j.mib.2015.04.007.
28. Matte C, Descoteaux A. 2016. Exploitation of the host cell membrane fusion machinery by *Leishmania* is part of the infection process. PLoS Pathog 12:e1005962. https://doi.org/10.1371/journal.ppat.1005962.
29. Matte C, Casgrain PA, Seguin O, Moradin N, Hong WJ, Descoteaux A. 2016. *Leishmania major* promastigotes evade LC3-associated phagocytosis through the action of GP63. PLoS Pathog 12:e1005690. https://doi.org/10.1371/journal.ppat.1005690.
30. Romano A, Carneiro MBH, Doria NA, Roma EH, Ribeiro-Gomes FL, Inbar E, Lee SH, Mendez J, Paun A, Sacks DL, Peters NC. 2017. Divergent roles for Ly6C$^+$CCR2$^+$CX3CR1$^+$ inflammatory monocytes during primary or secondary infection of the skin with the intra-phagosomal pathogen *Leishmania major*. PLoS Pathogens 13:e1006479. https://doi.org/10.1371/journal.ppat.1006479.
31. Terrazas C, Varikuti S, Oghumu S, Steinkamp HM, Ardic N, Kimble J, Nakhasi H, Satoskar AR. 2017. Ly6C(hi) inflammatory monocytes promote susceptibility to *Leishmania donovani* infection. Sci Rep 7:14693. https://doi.org/10.1038/s41598-017-14935-3.
32. Hammami A, Abidin BM, Charpentier T, Fabie A, Duguay AP, Heinonen KM, Stager S. 2017. HIF-1alpha is a key regulator in potentiating suppressor activity and limiting the microbicidal capacity of MDSC-like cells during visceral leishmaniasis. PLoS Pathog 13:e1006616. https://doi.org/10.1371/journal.ppat.1006616.

33. Foote JR, Patel AA, Yona S, Segal AW. 2019. Variations in the phagosomal environment of human neutrophils and mononuclear phagocyte subsets. Front Immunol 10:188. https://doi.org/10.3389/fimmu.2019.00188.
34. Lauvau G, Chorro L, Spaulding E, Soudja SM. 2014. Inflammatory monocyte effector mechanisms. Cell Immunol 291:32–40. https://doi.org/10.1016/j.cellimm.2014.07.007.
35. Burton NA, Schurmann N, Casse O, Steeb AK, Claudi B, Zankl J, Schmidt A, Bumann D. 2014. Disparate impact of oxidative host defenses determines the fate of *Salmonella* during systemic infection in mice. Cell Host Microbe 15:72–83. https://doi.org/10.1016/j.chom.2013.12.006.
36. Sampath P, Moideen K, Ranganathan UD, Bethunaickan R. 2018. Monocyte subsets: phenotypes and function in tuberculosis infection. Front Immunol 9:1726. https://doi.org/10.3389/fimmu.2018.01726.
37. Serbina NV, Shi C, Pamer EG. 2012. Monocyte-mediated immune defense against murine *Listeria monocytogenes* infection. Adv Immunol 113:119–134. https://doi.org/10.1016/B978-0-12-394590-7.00003-8.
38. Bedard K, Krause KH. 2007. The NOX family of ROS-generating NADPH oxidases: physiology and pathophysiology. Physiol Rev 87:245–313. https://doi.org/10.1152/physrev.00044.2005.
39. Vieira OV, Botelho RJ, Grinstein S. 2002. Phagosome maturation: aging gracefully. Biochem J 366:689–704. https://doi.org/10.1042/BJ20020691.
40. Vinet AF, Fukuda M, Turco SJ, Descoteaux A. 2009. The *Leishmania donovani* lipophosphoglycan excludes the vesicular proton-ATPase from phagosomes by impairing the recruitment of synaptotagmin V. PLoS Pathog 5:e1000628. https://doi.org/10.1371/journal.ppat.1000628.
41. da Silva Vieira T, Arango Duque G, Ory K, Gontijo CM, Soares RP, Descoteaux A. 2019. *Leishmania braziliensis*: strain-specific modulation of phagosome maturation. Front Cell Infect Microbiol 9:319. https://doi.org/10.3389/fcimb.2019.00319.
42. Olivier M, Atayde VD, Isnard A, Hassani K, Shio MT. 2012. *Leishmania* virulence factors: focus on the metalloprotease GP63. Microbes Infect 14:1377–1389. https://doi.org/10.1016/j.micinf.2012.05.014.
43. Descoteaux A, Turco SJ. 1999. Glycoconjugates in *Leishmania* infectivity. Biochim Biophys Acta 1455:341–352. https://doi.org/10.1016/s0925-4439(99)00065-4.
44. Isnard A, Shio MT, Olivier M. 2012. Impact of *Leishmania* metalloprotease GP63 on macrophage signaling. Front Cell Infect Microbiol 2:72. https://doi.org/10.3389/fcimb.2012.00072.
45. Podinovskaia M, Descoteaux A. 2015. *Leishmania* and the macrophage: a multifaceted interaction. Future Microbiol 10:111–129. https://doi.org/10.2217/fmb.14.103.
46. Peters NC, Egen JG, Secundino N, Debrabant A, Kimblin N, Kamhawi S, Lawyer P, Fay MP, Germain RN, Sacks D. 2008. *In vivo* imaging reveals an essential role for neutrophils in leishmaniasis transmitted by sand flies. Science 321:970–974. https://doi.org/10.1126/science.1159194.
47. Ribeiro-Gomes FL, Roma EH, Carneiro MB, Doria NA, Sacks DL, Peters NC. 2014. Site-dependent recruitment of inflammatory cells determines the effective dose of *Leishmania major*. Infect Immun 82:2713–2727. https://doi.org/10.1128/IAI.01600-13.
48. Chaves MM, Lee SH, Kamenyeva O, Ghosh K, Peters NC, Sacks D. 2020. The role of dermis resident macrophages and their interaction with neutrophils in the early establishment of *Leishmania major* infection transmitted by sand fly bite. PLoS Pathog 16:e1008674. https://doi.org/10.1371/journal.ppat.1008674.
49. Lam GY, Huang J, Brumell JH. 2010. The many roles of NOX2 NADPH oxidase-derived ROS in immunity. Semin Immunopathol 32:415–430. https://doi.org/10.1007/s00281-010-0221-0.
50. Segal AW. 2005. How neutrophils kill microbes. Annu Rev Immunol 23:197–223. https://doi.org/10.1146/annurev.immunol.23.021704.115653.
51. Plewes KA, Barr SD, Gedamu L. 2003. Iron superoxide dismutases targeted to the glycosomes of *Leishmania chagasi* are important for survival. Infect Immun 71:5910–5920. https://doi.org/10.1128/iai.71.10.5910-5920.2003.
52. Davenport BJ, Martin CG, Beverley SM, Orlicky DJ, Vazquez-Torres A, Morrison TE. 2018. SODB1 is essential for *Leishmania major* infection of macrophages and pathogenesis in mice. PLoS Negl Trop Dis 12:e0006921. https://doi.org/10.1371/journal.pntd.0006921.
53. Levick MP, Tetaud E, Fairlamb AH, Blackwell JM. 1998. Identification and characterisation of a functional peroxidoxin from *Leishmania major*. Mol Biochem Parasitol 96:125–137. https://doi.org/10.1016/s0166-6851(98)00122-4.
54. Henard CA, Carlsen ED, Hay C, Kima PE, Soong L. 2014. *Leishmania amazonensis* amastigotes highly express a tryparedoxin peroxidase isoform that increases parasite resistance to macrophage antimicrobial defenses and fosters parasite virulence. PLoS Negl Trop Dis 8:e3000. https://doi.org/10.1371/journal.pntd.0003000.
55. Pham NK, Mouriz J, Kima PE. 2005. *Leishmania pifanoi* amastigotes avoid macrophage production of superoxide by inducing heme degradation. Infect Immun 73:8322–8333. https://doi.org/10.1128/IAI.73.12.8322-8333.2005.
56. Luz NF, Andrade BB, Feijo DF, Araujo-Santos T, Carvalho GQ, Andrade D, Abanades DR, Melo EV, Silva AM, Brodskyn CI, Barral-Netto M, Barral A, Soares RP, Almeida RP, Bozza MT, Borges VM. 2012. Heme oxygenase-1 promotes the persistence of *Leishmania chagasi* infection. J Immunol 188:4460–4467. https://doi.org/10.4049/jimmunol.1103072.
57. Saha S, Basu M, Guin S, Gupta P, Mitterstiller AM, Weiss G, Jana K, Ukil A. 2019. *Leishmania donovani* exploits macrophage heme oxygenase-1 to neutralize oxidative burst and TLR signaling-dependent host defense. J Immunol 202:827–840. https://doi.org/10.4049/jimmunol.1800958.
58. Canton J, Khezri R, Glogauer M, Grinstein S. 2014. Contrasting phagosome pH regulation and maturation in human M1 and M2 macrophages. Mol Biol Cell 25:3330–3341. https://doi.org/10.1091/mbc.E14-05-0967.
59. Jesaitis AJ, Buescher ES, Harrison D, Quinn MT, Parkos CA, Livesey S, Linner J. 1990. Ultrastructural localization of cytochrome b in the membranes of resting and phagocytosing human granulocytes. J Clin Invest 85:821–835. https://doi.org/10.1172/JCI114509.
60. Johansson A, Jesaitis AJ, Lundqvist H, Magnusson KE, Sjolin C, Karlsson A, Dahlgren C. 1995. Different subcellular localization of cytochrome b and the dormant NADPH-oxidase in neutrophils and macrophages: effect on the production of reactive oxygen species during phagocytosis. Cell Immunol 161:61–71. https://doi.org/10.1006/cimm.1995.1009.
61. Dingjan I, Linders PT, van den Bekerom L, Baranov MV, Halder P, Ter Beest M, van den Bogaart G. 2017. Oxidized phagosomal NOX2 complex is replenished from lysosomes. J Cell Sci 130:1285–1298. https://doi.org/10.1242/jcs.196931.
62. Casbon AJ, Allen LA, Dunn KW, Dinauer MC. 2009. Macrophage NADPH oxidase flavocytochrome B localizes to the plasma membrane and Rab11-positive recycling endosomes. J Immunol 182:2325–2339. https://doi.org/10.4049/jimmunol.0803476.
63. Bayraktutan U, Blayney L, Shah AM. 2000. Molecular characterization and localization of the NAD(P)H oxidase components gp91-phox and p22-phox in endothelial cells. Arterioscler Thromb Vasc Biol 20:1903–1911. https://doi.org/10.1161/01.atv.20.8.1903.
64. Blanchette J, Racette N, Faure R, Siminovitch KA, Olivier M. 1999. *Leishmania*-induced increases in activation of macrophage SHP-1 tyrosine phosphatase are associated with impaired IFN-gamma-triggered JAK2 activation. Eur J Immunol 29:3737–3744. https://doi.org/10.1002/(SICI)1521-4141(199911)29:11<3737::AID-IMMU3737>3.0.CO;2-S.
65. S CK, Cook ECL, Hernandez-Garcia E, Martinez-Lopez M, Conde-Garrosa R, Iborra S. 2020. SHP-1 regulates antigen cross-presentation and is exploited by *Leishmania* to evade immunity. Cell Rep 33:108468. https://doi.org/10.1016/j.celrep.2020.108468.
66. Ding Y, Guo Z, Liu Y, Li X, Zhang Q, Xu X, Gu Y, Zhang Y, Zhao D, Cao X. 2016. The lectin Siglec-G inhibits dendritic cell cross-presentation by impairing MHC class I-peptide complex formation. Nat Immunol 17:1167–1175. https://doi.org/10.1038/ni.3535.
67. Lodge R, Descoteaux A. 2008. *Leishmania* invasion and phagosome biogenesis. Subcell Biochem 47:174–181. https://doi.org/10.1007/978-0-387-78267-6_14.
68. Polando R, Dixit UG, Carter CR, Jones B, Whitcomb JP, Ballhorn W, Harintho M, Jerde CL, Wilson ME, McDowell MA. 2013. The roles of complement receptor 3 and Fcgamma receptors during *Leishmania* phagosome maturation. J Leukoc Biol 93:921–932. https://doi.org/10.1189/jlb.0212086.
69. Gupta N, Goyal N, Rastogi AK. 2001. *In vitro* cultivation and characterization of axenic amastigotes of *Leishmania*. Trends Parasitol 17:150–153. https://doi.org/10.1016/s1471-4922(00)01811-0.
70. Zilberstein D. 2020. *In vitro* culture for differentiation simulation of *Leishmania* spp. Methods Mol Biol 2116:39–47. https://doi.org/10.1007/978-1-0716-0294-2_3.
71. Prive C, Descoteaux A. 2000. *Leishmania donovani* promastigotes evade the activation of mitogen-activated protein kinases p38, c-Jun N-terminal kinase, and extracellular signal-regulated kinase-1/2 during infection of naive macrophages. Eur J Immunol 30:2235–2244. https://doi.org/10.1002/1521-4141(2000)30:8<2235::AID-IMMU2235>3.0.CO;2-9.
72. Scianimanico S, Desrosiers M, Dermine JF, Meresse S, Descoteaux A, Desjardins M. 1999. Impaired recruitment of the small GTPase rab7 correlates with the inhibition of phagosome maturation by *Leishmania donovani* promastigotes. Cell Microbiol 1:19–32. https://doi.org/10.1046/j.1462-5822.1999.00002.x.

73. Lazaro-Souza M, Matte C, Lima JB, Arango Duque G, Quintela-Carvalho G, de Carvalho Vivarini A, Moura-Pontes S, Figueira CP, Jesus-Santos FH, Gazos Lopes U, Farias LP, Araujo-Santos T, Descoteaux A, Borges VM. 2018. *Leishmania infantum* lipophosphoglycan-deficient mutants: a tool to study host cell-parasite interplay. Front Microbiol 9:626. https://doi.org/10.3389/fmicb.2018.00626.
74. Holm A, Tejle K, Magnusson KE, Descoteaux A, Rasmusson B. 2001. *Leishmania donovani* lipophosphoglycan causes periphagosomal actin accumulation: correlation with impaired translocation of PKCalpha and defective phagosome maturation. Cell Microbiol 3:439–447. https://doi.org/10.1046/j.1462-5822.2001.00127.x.
75. Joshi PB, Kelly BL, Kamhawi S, Sacks DL, McMaster WR. 2002. Targeted gene deletion in *Leishmania major* identifies leishmanolysin (GP63) as a virulence factor. Mol Biochem Parasitol 120:33–40. https://doi.org/10.1016/s0166-6851(01)00432-7.
76. Button LL, Reiner NE, McMaster WR. 1991. Modification of GP63 genes from diverse species of *Leishmania* for expression of recombinant protein at high levels in *Escherichia coli*. Mol Biochem Parasitol 44:213–224. https://doi.org/10.1016/0166-6851(91)90007-s.
77. Arango Duque G, Jardim A, Gagnon É, Fukuda M, Descoteaux A. 2019. The host cell secretory pathway mediates the export of *Leishmania* virulence factors out of the parasitophorous vacuole. PLoS Pathog 15:e1007982. https://doi.org/10.1371/journal.ppat.1007982.
78. Spath GF, Beverley SM. 2001. A lipophosphoglycan-independent method for isolation of infective *Leishmania* metacyclic promastigotes by density gradient centrifugation. Exp Parasitol 99:97–103. https://doi.org/10.1006/expr.2001.4656.
79. Arango Duque G, Fukuda M, Descoteaux A. 2013. Synaptotagmin XI regulates phagocytosis and cytokine secretion in macrophages. J Immunol 190:1737–1745. https://doi.org/10.4049/jimmunol.1202500.